15th IMEKO TC10 Workshop on Technical Diagnostics
Technical Diagnostics in Cyber-Physical Era
Budapest, Hungary, June 6-7, 2017

State parameter estimation of lead-acid battery pack using impulse excitation method

Bence Csomos[1], Gabor Kohlrusz[2], Dr. Denes Fodor[3]

[1] University of Pannonia, Department of Automotive Mechatronics
csomosb@almos.uni-pannon.hu
[2] University of Pannonia, Department of Automotive Mechatronics
kohlruszg@almos.uni-pannon.hu
[3] University of Pannonia, Department of Automotive Mechatronics
fodor@almos.uni-pannon.hu

***Abstract* – This paper describes an analysis of impulse excitation method to determine initial parameters of lead-acid battery model. The initial model parameters are essential inputs of state predictors and significantly influence the precision of SoC and SoH tracking.**
Two types of Randles-model have been introduced where the model parameters were exploited from the impulse excited voltage response of a battery.
Current impulse excitation approach is resource-saving and convenient way to generate excitation signal by for example, switching relays especially in automotive systems. Switching a relay through a load causes a squarewave-like change in the battery current. Either is a load current or charging current, the battery's voltage response depends on the actual battery's SoC and SoH. Using the discharge stages of voltage response characteristic of an Exide 15Ah AGM type battery, resistive and capacitive components of the battery model has been determined. The proposed model and method show promising results to set the initial parameters for state estimators.

I. INTRODUCTION

In our daily life, the number of mobile devices and utilities, that can operate without grid connections, increases. Even though Li batteries have better performance properties and energy indicators, lead-acid batteries are still cheaper, significantly present in commercial applications and almost fully recyclable. Therefore, any development on lead-acid battery systems are still obligate.

State prediction is essential to operate energy storages comfortably and in reliable conditions. In long-term usage, their operation mode has an influence on the energy storage's lifespan, efficiency, safety, economy and it cannot exceed certain technology limits

The fundamental state parameters of electrochemical energy storages are the State-of-Charge (SoC), State-of-Health (SoH) and State-of-Function (SoF) while environment temperature, load/charge current, charge/discharge voltage and charge cycle are still important factors.

Several methods exist in order to determine SoC and SoH. According to [1], Discharge Test, Coulomb-Counting, Open-Circuit Voltage Method, Coup-de-Fouet Method, Linear Function Regression, Electrochemical Impedance Spectroscopy (EIS), Inner Resistance Method and *Model Based State Estimators* are relevant. Even several battery type exists like Li-ion, Li-polymer, lead-acid, Ni-MH or NiCd batteries, Randles battery models, tools and procedures to estimate state parameters are very similar to each other. [10] [12.]

The advantages of state estimators such as fast, realtime computation, adaptability to changes and long-term precision facilitate the model based methods dominating in on-line automotive applications.

II. CURRENT IMPULSE EXCITATION METHOD

The model based estimator consists of two main parts:

- determining initial parameters
- tuning parameters

EIS method is widespread in off-line initial parameter estimation, however, it is too time-consuming and require lab-fine measuring environment.

Generation of excitation signal is robust and convenient by switching relays and also, data acquisition and interaction with battery power net need simple circuitry. Impulses can be indirectly utilized from the vehicle's power net for example, during ignition. [11.]

According to [5.] and [6.], the voltage response characteristic of a battery correlates with the battery's SoC, SoH and SoF.

The implementation process of current impulse

excitation method consists of main 3 steps:

- Measuring and establishing a battery model
- Determining initial model parameters
- Implementing parameter estimator system for parameter tuning

In the first and second step, an improved Randles battery model is created bearing in mind a compromise between computation time and battery chemical details.

In the second step, load current is applied on the battery and voltage, current and battery/ambient temperature are monitored and logged. Using a minimalizing algorithm, model functions fit to the measured voltage data. Initial model parameters can be derived from the fit functions.

The third step introduces a model based parameter estimator to tune the model parameters to track changes in battery current, SoC, SoH and temperature.

III. LEAD-ACID BATTERY MODEL

A typical dynamic battery model is based on the Randles-model. [2.] It represents the battery's simplified electrochemistry only for electrode and bulk regions. Fig 1. shows the battery model that is extended by the battery's R_d self-discharge resistance. R_s is the serial resistance due to cell interconnections and electrolyte resistance. C_{dl} is the double-layer capacity connected parallel with R_{ct} charge-transfer resistance. C_b represents the battery's open-circuit voltage and the main charge storage. U_0 is the terminal voltage of the battery.

U_{dl} and U_b are the voltages through the C_{dl} and C_b capacitors, respectively.

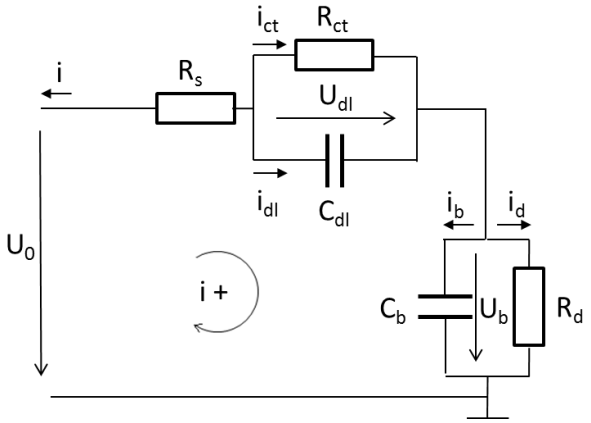

Fig. 1 Improved Randles-model of lead-acid battery

Using Kirchoff I - II. laws on each subsystem of RC components, the i output current can be written according to Eq 1.

$$i = -C_{dl}\frac{dU_{dl}}{dt} - -\frac{U_{dl}}{R_{ct}} = -C_b\frac{dU_b}{dt} - \frac{U_b}{R_d} \tag{1}$$

$$-R_{ct}C_{dl}\frac{dU_{dl}}{dt} - U_{dl} = R_{ct}i \tag{2}$$

$$-R_dC_b\frac{dU_b}{dt} - U_b = R_di \tag{3}$$

Considering Eq. 2. and Eq 3. state-space representation can be written in the form of Eq 4.

$$\frac{d}{dt}\begin{bmatrix}U_{dl}\\U_b\end{bmatrix} = \begin{bmatrix}-\frac{1}{R_{ct}C_{dl}} & 0\\ 0 & -\frac{1}{R_dC_b}\end{bmatrix}\begin{bmatrix}U_{dl}\\U_b\end{bmatrix} + \begin{bmatrix}-\frac{1}{C_{dl}}\\-\frac{1}{C_b}\end{bmatrix}i \tag{4}$$

$$U = \begin{bmatrix}1 & 1\end{bmatrix}\begin{bmatrix}U_{dl}\\U_b\end{bmatrix} + R_si \tag{5}$$

Time constants can be introduced for the product of $R_{ct}C_{dl}$ and R_dC_b. that is shown in Eq. 6. and Eq. 7. respectively.

$$\tau_b = R_dC_b \tag{6}$$

$$\tau_{dl} = R_{ct}C_{dl} \tag{7}$$

Introducing impulse input (Eq. 8), battery output (terminal voltage) can be written in the form of Eq. 11. using Eq. 9 and Eq. 10.

$$i(t) = i_0 1(t) \tag{8}$$

$$U_{dl}(t) = U_{dl0}e^{-\frac{t}{\tau_{dl}}} - R_{ct}i_0 1(t)\left(1 - e^{-\frac{t}{\tau_{dl}}}\right), \quad U_{dl}(0) = U_{dl0} \tag{9}$$

$$U_b(t) = U_{b0}e^{-\frac{t}{\tau_b}} - R_di_0 1(t)\left(1 - e^{-\frac{t}{\tau_b}}\right), \quad U_b(0) = U_{b0} \tag{10}$$

$$U = U_{dl0}e^{-\frac{t}{\tau_{dl}}} - R_{ct}i_0 1(t)\left(1 - e^{-\frac{t}{\tau_{dl}}}\right) + U_{b0}e^{-\frac{t}{\tau_b}} - R_di_0 1(t)\left(1 - e^{-\frac{t}{\tau_b}}\right) + R_si(t) \tag{11}$$

The Eq 11. output equation can be simplefied by grouping parameters. It leads to Eq. 12.

$$U(t) = Ae^{-\frac{t}{\tau_{dl}}} + Be^{-\frac{t}{\tau_b}} + C + D \quad (12)$$

U_{dl0} and U_{b0} in Eq. 11. related to the battery initial voltages that represents the quasi-initial battery charge in every discharge cycle by Eq. 13.

Under charge/discharge process, battery actual charge changes and the amount of the charge change can be theoretically determined by Eq. 14. More practical way to track charge changes is to use Eq. 15. utilizing charge/discharge current for battery remaining charge computation.

$$SoC(0) = Q_0 = C_s U_{s0} + C_b U_{b0} \quad (13)$$

$$SoC(t) = Q(t) = C_s U_s + C_b U_b \quad (14)$$

$$SOC(t) = Q(t) = \\ = SOC(0) \pm \frac{1}{C_s + C_b} \int_{t_0}^{t} (i_{batt}(\tau) \mp i_{loss}(\tau)) d\tau \quad (15)$$

Sign of the integration in Eq. 15. is minus in case of discharge and plus if the battery is under charge process. Eq. 12. is the model function in which the A, B, C, D, τ_{dl}, and τ_b determined by function regression and minimising algorithm for effective SoC tracking.

Model parameter A and τ_{dl} in Eq. 12. can be derived from regression on the excitation cycles and give fast estimation of resultant R_{ct}, C_{dl} and R_s values, however, in order to determine the rest of the Eq. 12. function parameters and receive more reliable results, long-term voltage characteristic needs to be evaluated.

Processing long-term (long time-constant) voltage data, the Randles-model (Fig. 1.) needs to be modified in order to get precise regression and precise R and C parameters derived.

Based on model on Fig 1., a modified Randles-model can be used to estimate long time-constant RC parameters according to the model function given by Eq. 16.

$$U(t) = Ae^{-\frac{t}{\tau_{dl}}} + \left[1 - Be^{-\frac{t}{\tau_b}}\right] - Ct + E_0 \quad (16)$$

where $Ae^{-\frac{t}{\tau_{dl}}}$ and $\left[1 - Be^{-\frac{t}{\tau_b}}\right]$ represents a short and a long time-constant RC tags, respectively, $-Ct$ is fit to the linear tail-region and E_0 introduces a voltage offset originating from the fully discharged AGM battery pack. E_0 is related to U_b as the resulted voltage of remaining charge stored in C_b. R_d isneeds to be considered as a part of the total polarization resistance since inner self-discharge resistance cannot be derived by impulse method so far.

In order to eliminate the residual error occuring in the early stage of Fig. 5., the simplefied Randles model given by Eq. 16. has been extended with an additional RC subsystem that introduces a detailed electrochemical battery model. The extra RC subsystem represents detailed polarization resistance and double-layer capacitance at both electrodes of the battery pack. [13.]

Fig. 2. shows the Extended Randles-model with an additional RC tag.

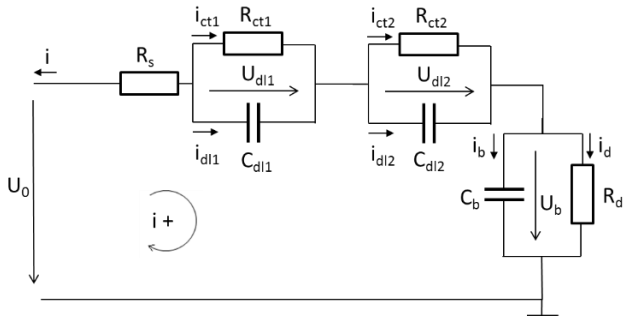

Fig. 2 Extended Randles-model with R_{ct2} and C_{dl2} subsystem to adapt to long time-constant discharge region

The model function for the Extended Randles-model can be writteng in the form of Eq. 17.

$$U(t) = Ae^{-\frac{t}{\tau_1}} - Be^{-\frac{t}{\tau_2}} + \left[1 - Ce^{-\frac{t}{\tau_3}}\right] - Ct + E_0 \quad (17)$$

Using proper constraints and initial parameters, a precise regression can be made and deriving long time-constant RC parameters becomes possible.

IV. MEASURING ENVIRONMENT

Data acquisition and logging were performed on a 10A test bench. The test bench consists of 2 main units that provide range extension between 0-1A and 1-10A currents. For lower currents, signal conditioning is needed to raise the signal from noise level therefore, a preamp, filter and buffer section has been designed to the board. Two different rheostats, one is 25W 1kΩ and one is 100W 5Ω, have been applied as loads. Currents are measured through a 100W 1Ω shunt resistor. Switching between load profiles can be made by relays. The test bench is integrated into a NI PXIe-1082 embedded system environment with PXI-6341 DAQ module. The supervisory and logging software has been implemented in LabVIEW 2013.

During the tests, an Exide 15Ah AGM battery has been inspected. In order to identify the battery normal discharge characteristics, 1 to 5A discharges were made

including different relaxation time following a full charge. Sampling time was set to 100ms. The battery was recharged after each discharge with an auxiliary CC/CV charger under C/10 charge current regulation.

Measurement data was evaluated in Matlab software platform. The processing software consists of file read, low frequency filtering, high frequency regression and RC parameter deduction from the regression function.

V. SMALL TIME-CONSTANT FUNCTION REGRESSION INITIALIZATION

As a current impulse excitation, a 3A load current has been chosen and the discharge was interrupted every 4s. It means that the discharge impulse width was 4s and it was followed by a 10s relaxation period. The impulse cycle was last for 1 hour. The results are shown on Fig. 4.

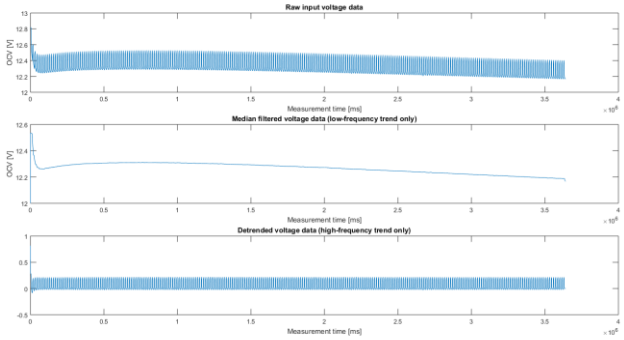

Fig. 3 1h long, 3A discharge current impulse characteristic (top), low-frequency filtering by Median-filter (middle) and detrended voltage data (bottom)

In detrended voltage data, only decaying voltage curves in discharging periods were analyzed. Thus, all of the curves of the load periods should be isolated first from the whole data and then, concatenated only the decaying curves after each other. In this case, not only each individual decays but also the trend of decays during the whole discharge process can show information about changes in SoC or SoH.

Regression has been made for each of the individual voltage decays using Matlab fmincon function. The error function is based on the least-square error that can be written in the form of Eq. 18.

$$e = \sum (y_{model} - y_{meas})^2 \tag{18}$$

The fit of the fit function and finding an optimum solution is greatly dependent on the initial values of optimization. Moreover, initial parameters should be set carefully because even the fit function fit smoothly onto the measurement points; R and C parameters derived from the fit function can lose physical meaning by gaining unreasonable signs or values. Based on several measurements, it can be stated that the initial value for short time constant should be of the same order of magnitude as one load period while the long time constant should be in a range of the whole measurement time. Table 1. summarizes the initial values. Also, constraining the optimization with lower or upper boundaries, can be eliminate the invalid or physically meaningless values of R and C parameters.

Applying short impulses whose impulse width is much smaller than the smallest time constant subsystem in the model allows to neglect the long-term terms in Eq. 12. and leads to Eq. 19. Evaluating only individual decaying curves simplifies the fit and lower the computation time, however, detecting long-term changes in the battery through B and C terms is not possible.

$$U(t) = Ae^{-\frac{t}{\tau_{dl}}} + D \tag{19}$$

B, τ_b and C parameters can be derived from a fit function of long time-constant section of the battery.

Table 1 Initial values of fit function

Fit function parameters	Initial values
A	1
τ_{dl}	4000
D	1

VI. LONG TIME-CONSTANT FUNCTION REGRESSION INITIALIZATION

Long time-constant RC parameters can be determined by regression using either Eq. 16 or Eq. 17.

First, the voltage characteristic needs to be filtered to suppress “impulse spikes”. Then, setting proper constraints and initial values of Eq. 16 and Eq. 17., function fit can be performed. Initial values and constraints for Eq. 16. fit are listed in Table 2.

Table 2 Constraints and initial values of modified Randles-model based on Eq. 16.

Fit parameters	Lower boundaries	Init values
A	0	0,5
τ_{dl}	0	11
B	0	1
τ_b	1000	9000
C	0	1
E_0	0	1

The constraints and initial values for Extended model fit is shown in Table 3.

Table 3 Constraints and initial values of Extended Randles-model based on Eq. 17.

Fit parameters	Lower boundaries	Init values
A	0	0,5
τ_1	0	11
B	0	1
τ_2	100	400
C	0	1
τ_3	2000	9000
D	0	1
E_0	0	1

VII. RESULTS

Running the regression on the concatenated small time-constant decaying curves with the initial parametes set in Table 1., it returns a P parameter vector and fit function. Using the set of estimated P parameter vector of fit function, average R and C value and changes in R and C can be determined. Derived average R and C values from evaluating small time-constant (impulse) regions are shown in Table 4.

Table 4 Derived model parameters of small time-constant region in Fig. 1 based on Eq. 19.

Fit function parameters	Initial values
$R_{ct_{avg}}$	0,0203 Ω
$R_{s_{avg}}$	0,1142 Ω
C_{dl}	$1{,}71 \cdot 10^5 F$

The long time-constant regression results can be seen on Fig. 5., using initial values and constraints listed in Table 2.

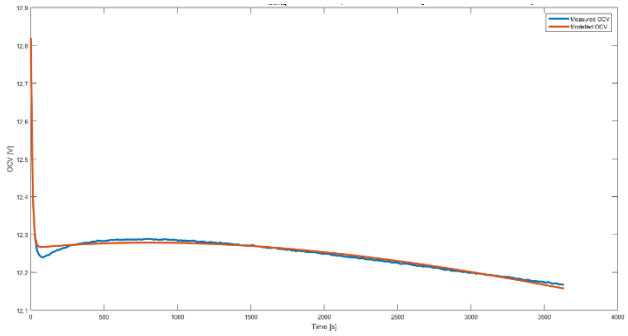

Fig. 4 Characteristics of long time-constant voltage measurement data and improved Randles-model based on Eq. 16. Measured voltage (blue line), Modeled voltage (red line)

On Fig. 5., it can be seen that a regression error occurs in the early stage of the voltage curve. Running an error estimation through the whole discharge profile, it gives 0.005 average error with 0,026 peak. (Fig. 6.)

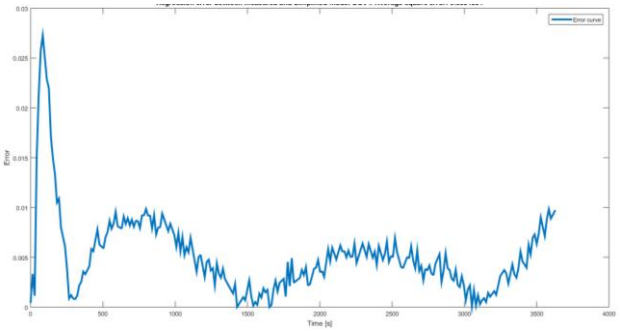

Fig. 5 Square error between the improved Randles-model and measurement voltage data

The Extended Randles-model, introduced in Section III. by Eq. 17., the residual error can be significantly decreased and peak-shaved by the extra RC tag. The regression results on the Extended Randles-model can be seen on Fig. 7. and derived parameters in Table 5.

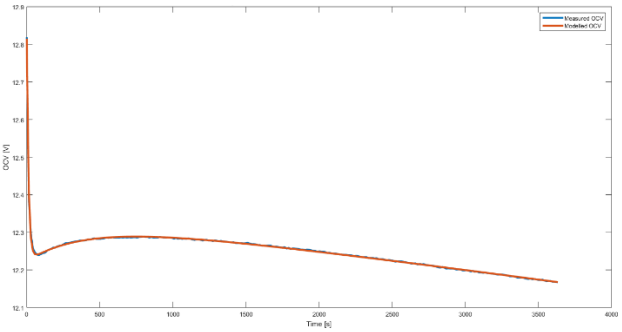

Fig. 6 Characteristics of long time-constant voltage measurement data and Extended Randles-model based on Eq 17.

Comparing the modeled and measured voltage characteristics (Fig. 8.), it can be seen that the average error does not exceed 0.001 and 0,014 peak.

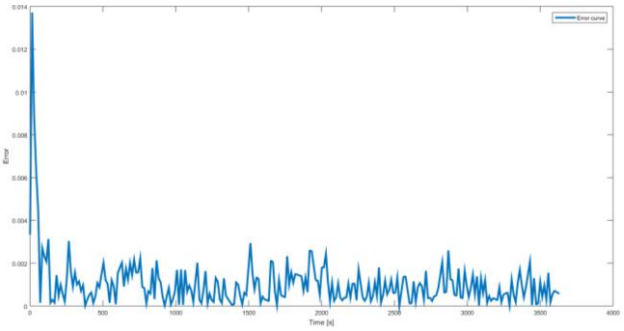

Fig. 7 Square error between the Extended Randles-model and measurement voltage data

Table 5 Derived parameters of Extended Randles Battery. model in Fig 2 based on Eq. 17.

Model parameters	Derived values
R_{ct1}	0,196 Ω
R_{ct2}	0,0385 Ω
R_d (related to polarization)	0,1595 Ω
R_s	0,3943 Ω
C_{dl1}	161,2 F
C_{dl2}	10400 F
C_b	81500 F
E_0	11,82 V

Both small and long time-constant model parameters are changing during a discharge and they strongly depend on the battery SoC, discharge current and temperature.

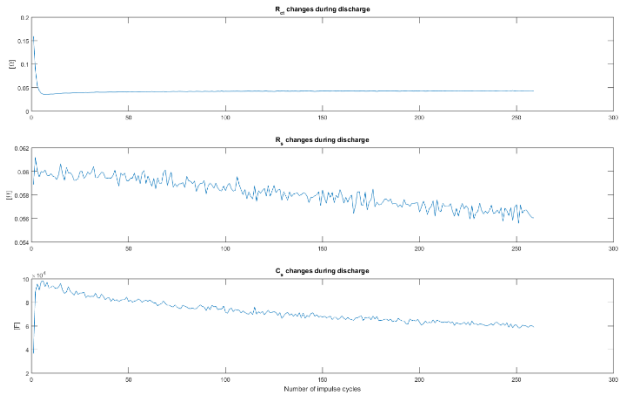

Fig. 8 Variation of model parameters during impulse discharge. R_{ct} (top), R_s (middle), C_{dl} (bottom)

VIII. CONCLUSIONS

In this paper, current impulse excitation has been analyzed to determine model parameters in Randles battery models for lead-acid battery. An Extended Randles-model has been developed in order to estimate complete RC battery model parameters and decrese residual error of modified Randles-models. Variation in RC values in battery models due to different discharge profiles have been analysed. Comparing the results with results expected in [10], it can be stated that variation in RC values can be linked to changes in discharge characteristics. the results show good utilization possibilities of current impulse based method to efficiently detect SoC changes in battery packs as well as in cells and also, to be efficiently used to serve initial parameters for state estimators.

IX. REFERENCES

[1.] Sabine Piller, Marion Perrin, Andreas Jossen, Methods for state-of-charge determination and their application, Journal of Power Sources 96, 113-120., 2001

[2.] Phillip E. Pascoe, Adnan H. Anbuky, The behavior of the coup de fouet of valve-regulated lead-acid batteries, Journal of Power Sources, 111, 304-319., 2002

[3.] Nihal Kularatna, Dynamics and modeling of rechargable batteries, IEEE Power Electronics Magazine, 2014

[4.] Yong-Duk Lee, Sung-Yeul Park, Soo-Bin Han, Online embedded impedance measurement using high-power battery charger, IEEE Transactions on industry applications, Vol.51., No.1., Jan/Feb. 2015.

[5.] Anahita Banaei, Babak Fahimi, Real time condition monitoring in Li-ion batteries via battery impulse response, IEEE, 2010.

[6.] Anahita Banaei, Amir Khoobroo, Babak Fahimi, Online detection of terminal voltage in Li-ion batteries via impulse response, IEEE, 2009.

[7.] B.S. Bhangu, P.Bentley, D.A. Stone, C.M. Bingham, Observer techniques for estimating the State-of-CHarge and State-of-Health of AGMBs for Hybrid Electric Vehicles, IEEE, 2005

[8.] Andreas Jossen, Fundamentals of battery dynamics, Journal of Power Sources 154, No. 530-538., 2006 (Indokolja: pozitív és negatív elektróda Cdl értékeinek intervallumai

[9.] Shing-Lih Wu, Hung-Cheng Chen, Shuo-Rong Chou, Fast estimation of State of Charge for Lithium-ion batteries, Energies, 7, 3438-3452, ISSN 1996-1073, 2014

[10.] P. Spagnol, S. Rossi, S. M. Savaresi, Kalman filter SoC estimation for Li-ion batteries, IEEE International Conference on Control Applications, Denver, 2011

[11.] Gábor Bárány, Lead-acid battery state detection for automotive electrical energy management, PhD thesis, University of Technology and Economics, Budapest, 2014

[12.] Lalitha Devarakonda, Haifeng Wang, Tingshu Hu, Parameter identification of circuit models for lead-acid batteries under non-zero initial conditions, American Control Conference, 4-6 June 2014, Portland, USA

[13.] Goran Kujundzic, Sandor Iles, Jadranko Matusko, Mario Vasak, Optimal charging of valve-regulated lead-acid batteries based on model predictive control, Elsevier, Applied Energy 187 (2017) 189-202